Study of the unusable liquid propellant residues evaporation processes parameters in the tanks of the launch vehicle expended stage in microgravity

V I Trushlyakov[1], V A Urbansky[1], N V Pustovoy[2]
[1]Omsk State Technical University, 11, Mira ave., Omsk, 644050, Russia
[2]Novosibirsk state technical University, 20, Marx prospect, Novosibirsk, Russia

Abstract. A method is proposed for studying the evaporation process of unusable rocket propellant (RP) residues in an expended stage (ES) under weightless conditions. Two options were considered as boundary conditions for liquid RP residues: a) liquid drop distribution in N identical drops, whose surface decreases during evaporation and b) the liquid distribution in the lower tank bottom and the mirror presence, whose area decreases during evaporation. A high-temperature stream of hydrogen peroxide decomposition products is used as a heat carrier (HC) fed to the fuel tank. The physical and mathematical model of the liquid evaporation process is based on the first thermodynamics law. Based on the analysis of the Frud and Grashof criteria, the assumption that there is no convection movement inside the drop (Rayleigh number is less than critical) for both boundary conditions variants, the heat transfer coefficient of the gas-vapor mixture (GVM) produced in the tank is determined due to the regression dependence obtained under ground conditions as a function of the Nusselt, Reynolds and Prandtl numbers. GVM parameters for the considered boundary conditions variants and the proposed physical mathematical model are compared with the results obtained earlier for the boundary conditions variant of uniform fluid distribution over the inner tank wall (third boundary conditions variant) and the boundary layer theory usage based on integral impulses, energy and diffusion ratios. The thermophysical GVM parameters and the GVM exhaust velocity for oxygen and kerosene are provided for two boundary conditions types, using the example of Soyuz-2.1.v type fuel tanks. The total mass of the RP residues evaporation system structure is less than 1.3% of the total “dry” ES design mass.

1. Introduction

To meet the requirements for reducing the technogenic impact of promising launch vehicles with main liquid rocket engines (LRE), in accordance with the recommendations adopted by the Inter-Agency Space Debris Coordination Committee (IADC) [1], it is necessary to completely eliminate unusable liquid RP residues in the ES tanks remaining at the orbits in near-earth space. The same requirement should be met for the ES, which return to the impact areas (off-shore, on-shore) located on the Earth surface after separation from the LV [2]. Currently, there exist some methods to reduce unusable RP residues in the ES tanks, for example, [3, 4]:

– individual RP working margin refueling in fuel LV tanks for a specific payload, but not for standard RP filling for various payloads;

– improving the operation accuracy of the starting propulsion equipment and the RP expenditure control system for the LV flight;

– applying the LV motion terminal control ensuring the complete depletion of a propellant component;

– minimizing insufficient propellant intake from the tank, warranty propellant load, etc.

A well-known method that provides a cardinal reduction of unusable RP residues, without making claims on other onboard LV systems, is a method based on convection heat and mass transfer in the ES tanks due to the hot gases supply to the tanks, for example, [5 - 9]. Analogous to this method are chemical propellant rockets tanks pressurization systems using self-igniting propellant components such as unsymmetrical dimethylhydrazine (UDMH) and nitric acid (NA) or nitrogen tetroxide (NT), during the LV flight along the powered ascent trajectory phase [10]. When dosed UDMH supply into the tank with NA / NT, a chemical RP interaction occurs with intensive heat release, leading to NA/NT evaporation and, accordingly, an increase in the pressurized gases pressure in the tank. A similar method is used in a tank with UDMH. However, the use of this method in case of non-self-igniting RP is difficult due to several reasons.

In works [5 - 8] for oxygen, kerosene RP supply system are considered as a separate constructive module. RP stocks for receiving HC are stored in separate tanks with a release system. To produce HC, autonomous gas generators (GG) installed outside the propellant tanks are used, and the tanks are fed with HC via individual lines. In work [9] propane is considered as a fuel, while RP residues in the tank O is an oxidizing agent, and in contrast to the works [5 - 8], the combustion was carried out directly in the ES tanks. If propane gas is used as fuel (F), and oxygen vapor as an oxidizer, they should be heated from –180°C to the propane gas burning temperature (–35°C), which requires powerful heaters of, respectively, volumes and masses. As a further development of this method, the use of hydrogen peroxide (HP) decomposition products supplied to O and F tanks, and its subsequent decomposition on the catalyst directly in the tanks, is proposed as a HC.

The essential characteristics of the RP residues evaporation system operation in the ES tanks is the factor of weightlessness that occurs after the main LRE is turned off. After turning off the main LRE occurs fluid continuity disruption. The experiments carried out in the microgravity tower showed possible variations in the fluid position, which is determined by the conditions for shutting down the LRE: a) an abrupt thrust discharge, b) the use of intermediate LRE thrust (transition to a smaller LRE thrust). In general, based on the numerous experiments analysis, three boundary conditions variants were adopted in [11]: a) the liquid location in the lower spherical bottom (when using the transition mode to a lower LRE thrust);

b) droplet liquid distribution in the tank volume (abrupt LRE thrust discharge, starting the brake engine, impact of the upper stage LRE jet, elastic lower bottom deformation from the loaded state to the initial state). In studies on the process of heat and mass transfer during liquids evaporation in microgravity [12–15], experimental data are presented showing a decrease in the heat transfer coefficient and recommendations to increase the heat exchange area to preserve heat transfer, for example, the evaporation of kerosene (aviation and common), at the same time: droplet sizes up to 1.53 mm, Reynolds numbers up to 8.86, temperatures in the range 573 - 674 K, blowing speeds up to 0.34 m / s.

Theoretical and experimental studies of convective heat and mass transfer in a model tank were carried out in [16] using the example of model fluid evaporation for various parameters of the heat carrier (air). A regressive dependence was set as a function of area change over time. This dependence had been obtained experimentally and approximated as a power polynomial.

The proposed evaporation system is the main component of the autonomous onboard descent system (AODS) of the expended LV stages from the launching trajectory. Its use as a part of the ES allows one to reduce the anthropogenic impact of the ES with liquid propellant rocket engines in impact areas while simultaneously increasing the mass of useful payload by removing restrictions on ES impact areas [7 – 9]. The structure of the AODS, except evaporation system, includes an ES navigation and motion control system, a telemetry system, and a power source [6, 9].

2. Statement of the problem

Using the example of tank O, it is necessary to develop a method for studying the parameters of the evaporation system of unusable liquid RP residues based on HP application, including:

- physical and mathematical model of the thermodynamic process of liquid RP residues evaporation when hydrogen peroxide is fed into the tank O with its subsequent catalytic decomposition;

- physical and mathematical model of HC, which is a high-temperature hydrogen peroxide (GVM_{HC}) decomposition products of;

- boundary conditions of the RP gas-vapor mixture in microgravity conditions, arising after shutdown of the LRE. Due to the fact that the evaporation processes of RP residues in tanks O, F are independent, the assumptions, the calculation scheme of thermal physical characteristics, and GVM_{HC} are the same. Therefore, mathematical models to evaluate the evaporation processes of liquid RP residues in the tanks O and F are the same as well.

3. Physical and mathematical model of the thermodynamic evaporation process on the example of liquid oxygen in the tank O

Based on the first thermodynamics law, the system of differential equations describing the thermodynamic process taking into account the participants in the process of heat and mass transfer, on the example of the tank O, is represented as [10]:

$$\begin{cases} \dfrac{dp}{dt} = \dfrac{k-1}{V}\left(i_g \dot{m}_g + i_{ev}\dot{m}_{ev} - i_{out}\dot{m}_{out} + \dfrac{dQ_\Sigma}{dt} \right), \\ \dfrac{d\rho}{dt} = \dfrac{1}{V}\left(\dot{m}_g + \dot{m}_{ev} - \dot{m}_{out} \right), \\ \dfrac{dT_w}{dt} = \dfrac{q_{rad}^{mix-w} + q_{con}^{mix-w} + q_{rad}^{w-lox} + q_{con}^{w-lox} - q_{rad}^{w}}{c_w \cdot m_w}, \\ \dfrac{dT_{mix}}{dt} = \dfrac{-q_{con}^{mix-w} - q_{rad}^{mix-w} - q_{rad}^{mix-lox} - q_{con}^{mix-lox} + q_{ev} - q_h^{mix-lox}}{c_{mix} \cdot m_{mix}}, \\ \dfrac{dT_{lox}}{dt} = \dfrac{q_{rad}^{mix-lox} + q_{con}^{mix-lox} - q_{rad}^{w-lox} - q_{con}^{w-lox} - q_{ev}}{c_{lox} \cdot m_{lox}}, \end{cases} \quad (1)$$

where $p, \rho, V, T_w, T_{mix}, T_{lox}$ are GVMo pressure in the O tank is, GVM density, tank volume, wall temperature, GVMo temperature, liquid oxygen temperature, respectively;

$\dot{m}_g, \dot{m}_{ev}, \dot{m}_{out}$ are mass-flow rate of HP, evaporated oxygen, at the outlet of the tank O, respectively;

i_g, i_{ev}, i_{out} are the enthalpies of HP, evaporated oxygen and GVMo leaving the tank;

$\frac{dQ_\Sigma}{dt}$ - the amount of heat released during the HP decomposition;

$c_w, c_{lox}, c_{mix}, m_w, m_{lox}, m_{mix}$ - are the heat capacity of the O tank wall, liquid oxygen, GVMo, as well as the masses of the tank O wall, liquid oxygen, and GVM, respectively;

q_{con}, q_{rad} are convective and radiant component between heat exchange participants;

q_{ev} is the heat of liquid oxygen evaporation;

is the radiant component of the HC, to the liquid surface:

$$q_{rad}^{mix-lox} = \sigma \varepsilon_{mix} F_{lox} \left(\left(\frac{T_{mix}(t)}{100} \right)^4 - \left(\frac{T_{lox}(t)}{100} \right)^4 \right) \quad (2)$$

F_{lox} is liquid surface area;

$q_{con}^{mix-lox}$ is the convective component of the HC, to the liquid surface;

$$q_{con}^{mix-lox} = \alpha_{mix} F_{lox} (T_{mix}(t) - T_{lox}(t)), \quad (3)$$

α_{mix} is the coefficient of heat transfer from HC to liquid:

$$\alpha_{mix} = \frac{\lambda_{mix} \cdot Nu_{mix}}{l}, \quad (4)$$

λ_{mix}, Nu_{mix} are thermal GVM conductivity (a pair of oxygen and helium supercharge gas) and the Nusselt number, respectively;

l is characteristic size, for this boundary conditions variant of oxygen in the O tank, the diameter of the tank is accepted;

T_{ev}, c_{lox} are evaporation temperature and heat capacity of liquid oxygen, respectively.

Assumptions are as follows:

– the initial conditions of liquid RP residues in the tank correspond to two options:

a) a mirror of the free liquid surface and b) in a gas-droplet state, while all the liquid is concentrated in N spherical droplets of the same size and distributed throughout the tanks volume, with each drop area decreasing in the course of RP evaporation (figure 1a, b);

– convective movement inside a drop of liquid and thermocapillary interaction are not considered, because the Rayleigh number for the considered conditions is less than the critical value; the size and, consequently, the drops number N is determined from their stability condition [17];

– the HP decomposition products leakage does not violate the integrity of the RP drops surface, and the tank height is taken as the characteristic size l.

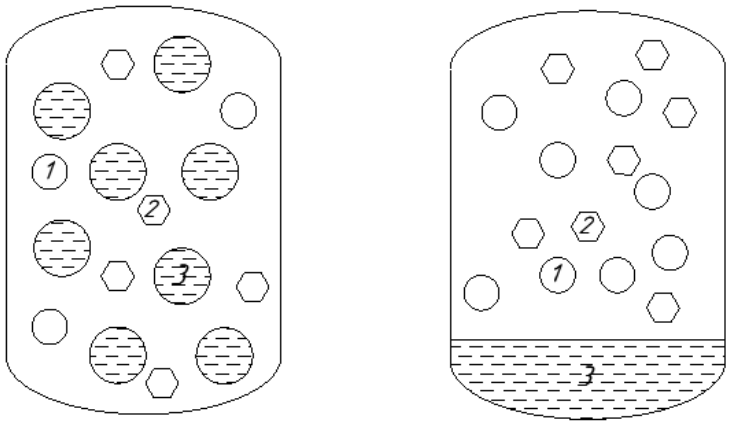

a) b)

Figure 1. The oxidizer location variants in the tank: a) the liquid is distributed over the tank volume in N drops of the same size, b) the liquid in the lower spherical tank bottom.
1 — oxygen in the gas phase, 2 — helium; 3 - liquid oxygen

4. Physical and mathematical models of GVM

According to the proposed technology of convective heat and mass transfer, two GVMs are formed in the evaporation system: a) GVMHC, that is the heat carrier in the form of hydrogen peroxide decomposition products forming a high-temperature gas-vapor mixture, consisting of 66% water vapor and 34% oxygen gas; b) GVMo, being a mixture of oxygen gas + gas pressurization helium + GVMHC from the tank O.

4.1 Physical and mathematical models of GVM_{HC}

Getting GVM_{HC} is carried out in a catalytic gas generator (GG) under the following conditions:

– the pressure at the outlet from the GG must be no less than the pressure in the tank, and the pressure inside the tank is greater than the pressure in the GG;

– exhaust velocity W_{HC} should ensure effective heat transfer from GVM_{HC} to liquid RP;

– GVM_{HC} temperature not less than 800°C;

– the operating time of the system for producing a HC is determined from the condition of liquid RP residues evaporation for a given time T_{giv}.

The mass second consumption of HP from the tank will be equal to that of GVM from GG and is determined from the condition for supplying a given amount of heat required for RP residues evaporation for a given time interval Tgiv.

For the tank O, is determined without consideration of the heat required to raise the oxygen temperature to the boiling point and helium gas temperature to the boiling point of oxygen, since at the beginning of the evaporation process, oxygen is in a state of boiling:

$$\dot{m}_{HC} = \dot{m}_{HP} = \frac{m_{\Sigma}^{o}}{T_{giv}} = \frac{m_{ox}^{odd} J_{ox} + (m_{he} c_{he} + m_{ox}^{vap} c_{ox}^{gas} + m_{ox}^{liq} c_{ox}^{liq})\Delta t}{T_{giv}}, \quad (5)$$

Where m_{Σ}^{o} is total reserves of hydrogen peroxide for the tank O to evaporate the liquid RP residues;

$m_{ox}^{odd}, J_{ox}, c_{ox}^{liq}$ are liquid residue mass, vaporization heat and heat capacity of oxygen;

$m_{ox}^{vap}, c_{ox}^{gas}$ are mass and heat capacity of oxygen vapor in the tank;

m_{he}, c_{he} are mass and heat capacity of helium in the tank;

Δt – temperature difference GVM in the tank and liquid oxygen.

The value of the nozzle area d_{HP} for the HP exhaust in GG is determined from the formula [18]:

$$\dot{m}_{HC} = \mu m \frac{\pi d_{HP}^{2}}{4} \phi \frac{p_2}{\sqrt{T_2}}, \quad (6)$$

where: μ - flow coefficient; p_2 - tank pressure with HP, T_2 - HP temperature in the tank.

ϕ - coefficient determined by the formula [18]:

$$\phi = \begin{cases} 1, & b \le b_{cr} \\ \sqrt{b^{2/k} - b^{k+1/k}}, & b > b_{cr} \end{cases}, b = \frac{p_s}{p_h}, b_{cr} = \left(\frac{2}{k+1}\right)^{\frac{k}{k-1}}, \quad (7)$$

the index h denotes the greater of the pressures (inside GG or in the tank), and the index s denotes the smaller one; k is GVMHC adiabatic index;

m - gas dynamic function is determined by the formula:

$$m = \begin{cases} \sqrt{2k/(k-1)R}, & b \le b_{cr} \\ \sqrt{k/R((2/k+1))^{(k+1)/(k-1)}}, & b > b_{cr} \end{cases} \quad (8)$$

R, k - specific gas constant (244 J/kgK) and GVM_{HC} adiabatic index (k = 1,4).

For the case under consideration (the ratio of pressures inside the tank with PV and GG $\gamma 1 = P_{GG}/P_{HP} = 6/7$) at k=1.4, the values b and b_{cr}, respectively, are equal to b_{cr} = 0,528, b = 0,833, m = 0,083, ϕ =0,198.

The GVM_{HC} exhaust velocity from GG in the tank W_{HC} is determined by the formula:

$$W_{HC} = \frac{4\dot{V}_{HC}}{\pi d_{GG}^{2}} \quad (9)$$

where: $\dot{V}_{mн}$ – the GVM_{HC} formation volumetric rate in GG is determined from the formula:

$$\dot{V}_{HC} = \dot{m}_{HP} / \rho_{GVM}^{HC}. \quad (10)$$

In the works [20, 21] the GVM_{HC} rates are given for various typical tank designs.

4.2 Physical and mathematical models of GVM_0

GVM_0 is a mixture of oxygen vapor and helium supercharging gas + GVM_{HC}. Physical and mathematical model of GVM_0 is determined by thermophysical parameters, which in turn depend on the rate at which oxygen vapor enters the volume of the O tank when the liquid phase of oxygen evaporates, GVM_{HC}

containing high-temperature water and oxygen vapor. The rate of oxygen mass evaporation from the surface is determined by the formula [19]:

$$\dot{m}_{ev} = \beta_p (p^* - p_{ox}) F_{lox}, \tag{11}$$

where p^* - the partial pressure of the evaporating oxygen at the liquid surface, tabular values from [22] are approximated in the form of a parabola:

$$p^* = A_0 + A_{1o} T + A_{2o} T^2 = 95.4 - 2.05 \cdot T + 0.011 \cdot T^2,$$

where: $A_{0,}$ $A_{1,}$ A_2 – coefficients for pressure approximation on the saturation line;

T – GVM_0 temperature;

Similarly, the partial kerosene pressure is determined by tabular values from [22]:

$$p^*_F = A_{0F} + A_{1F} T + A_{2F} T^2 = 7,07 \cdot 10^5 - 4641 \cdot T + 7,722 \cdot T^2,$$

where $A_{0,}$ $A_{1,}$ A_2 are approximation coefficients for pressure on the saturation line;

T – GVM_0/ GVM_k temperature;

p_{ox} is current partial oxygen vapor pressure in the free volume of the tank O;

F_{lox} is time-varying liquid oxygen surface area;

β_p is mass transfer coefficient is determined by the formula [12]:

$$\beta_p = \frac{\alpha}{c_{lox} \cdot \gamma \cdot T_{lox} \cdot R_{lox}}, \tag{12}$$

where $\alpha, c_{lox}, \gamma, T_{lox}, R_{lox}$ are heat transfer coefficient, specific heat capacity, specific gravity, temperature and specific gas constant of liquid oxygen, respectively.

The heat transfer coefficient value α_{mix} in (6) determined by the formula [23]:

$$\alpha_{mix} = \frac{\lambda_{mix} \cdot Nu_{mix}}{l}, \tag{13}$$

where:

l is characteristic size;

λ_{mix} is GVM_0 thermal conductivity;

$$Nu_{mix} = C_1 \cdot \mathrm{Re}_{mix}^{0,8} \cdot \mathrm{Pr}_{mix}^{0,43}, \tag{14}$$

$\mathrm{Re}_{mix}, \mathrm{Pr}_{mix}$ are Reynolds and Prandtl numbers for GVM_0, respectively.

Coefficient C_1 is determined by analyzing the obtained experimental and calculated data and for the considered variant with $Re > 5 \cdot 10^3$ accepted $C_1 = 0,037$ [23].

The expression for the Nusselt number (15) was obtained as a result of regression analysis performed on numerous ground-based experiments, and the possibility to use it for the considered conditions of convective heat transfer requires additional analysis with appropriate criteria.

The Frud and Grashof criteria analysis, which characterize the heat exchange processes similarity, shows that these criteria ratio for ground conditions and at flight altitude ES (h_1 < 400 km) equal to the ratio of the earth's field accelerations the at a height of h1 and the earth surface h_0, $g_0/g_1 = (r_0+h_1/r_o)^2 \sim 1$, r_0 = 6371 km – Earth radius.

Other evaluation criteria for the thermogravitational convection mechanism under microgravity are the Marangoni and Rayleigh criteria, which show the possibility of convective motions in a liquid as a result of a change in the liquid surface tension due to uneven heating. For this case under consideration, there is no possibility of convective motions in the liquid, since Rayleigh criterion is less than the critical value (the condition for the convective flows occurrence inside the liquid) [17].

The analysis performed shows the possibility of using the regression formula for calculating the Nusselt number (15) for the weightlessness conditions and the fluid boundary conditions of the two options shown in figure 1 a, b.

The vapor partial pressure current value p_{ox} in the free O tank volume at the current time in (12) is determined from [23] by the formula:

$$p_{ox} = \frac{R_{ox} T_{mix} (m_{ox} + \dot{m}_{ev} \cdot t)}{V(t)}, \quad (15)$$

where:

R_{ox} is oxygen vapor specific gas constant, J/kg·K;

$V(t)$ is current free tank volume, m^3;

m_{ox} is the gaseous oxygen initial mass in the O tank, kg;

When the GVM_0 is reset through the pressure dump valve, the vapor partial pressure current value p_{ox} in the O tank is determined by the formula:

$$p_{ox} = \frac{R_{ox} T_{mix} (m_{ox} + \dot{m}_{ev} \cdot t - \dot{m}_1 t)}{V(t)}, \quad (16)$$

where $\dot{m}_1$ is the mass second oxygen consumption when the GVM_0 is discharged from the O tank, which is ~ 73% of the total mass of the GVM_0..

Taking into account equation (12) and (16), the mass evaporation rate is [10]:

$$\dot{m}_{ev} = \frac{\beta_p F_{lox} (p^* - \frac{R_{ox} T(t) m_{ox}}{V})}{1 + \frac{\beta_p F_{lox} R_{ox} T(t) t}{V}}, \quad (17)$$

where:

p^* is partial pressure of the evaporating oxygen at the liquid surface, taken as equal to the saturated vapours pressure at the surface temperature $p^* = 0{,}13 МПа$, at the temperature of liquid surface evaporation of 90 K according to tabular values [22];

m_{ox} – the gaseous oxygen phase initial mass, kg; V – tank volume, m^3;

$F_{lox}(t)$ – the current fluid mirror surface area, m^2.

In accordance with the control algorithm of the evaporation system, the GVM pressure dump valve opens when the pressure in the O tank is reached. The pressure magnitude is determined by the tank strength from loading by internal GVM_0 pressure p_{valid}^{max}. GVM0 pressure dump valve is closed when the pressure determined by the dynamic strength is reached. The magnitude of this pressure is determined by the atmospheric free-stream external dynamic pressure p_{valid}^{ext}.

Graphs of changes in heat capacity, thermal conductivity and heat transfer during evaporation are shown in figure 2. Differences from [20] are due to the presence of a pressure gain section in the tanks O, F with subsequent discharge.

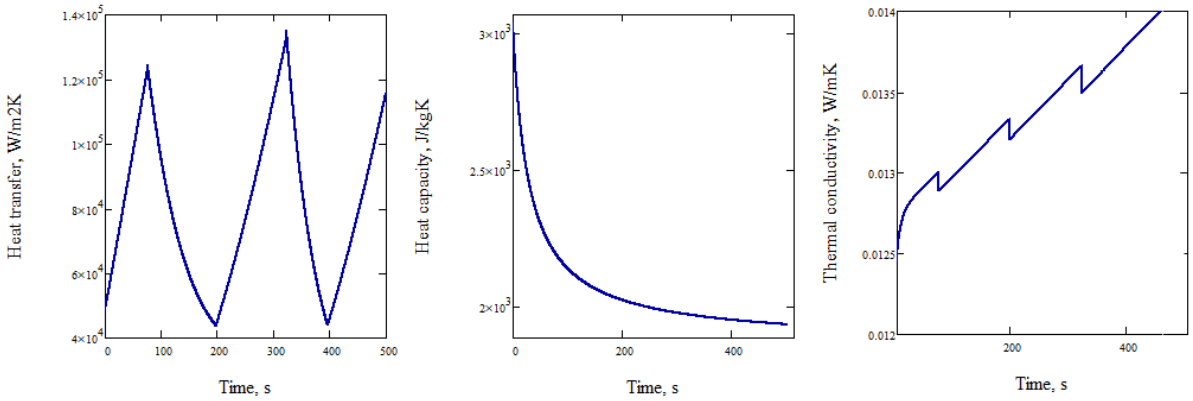

a) b) c)

Figure 2. Graphs of changes in GVM0 heat transfer, heat capacity and thermal conductivity in the tanks O for the boundary condition “mirror”.

As follows from the above results in figure 2:

– the GVM_0 heat transfer coefficient (figure 2a) has similar character of change due to the large effect of pressure on the heat transfer coefficient in accordance with [19];

– the GVM_0 heat capacity coefficient (figure 2b) depends on the ratio of the products mass fractions included in GVM_0 (oxygen, water vapor, helium) and in terms of the evaporation process time it approaches the mixture component (oxygen) heat capacity, which has the largest mass fraction;

– the GVM_0 thermal conductivity coefficient (figure 2c) depends on the temperature GVM_0 and pressure to a greater extent.

Figure 3 a, b shows the changes in pressure in tanks a) O and b) F – for 2 boundary conditions types (figure 1 a, b).

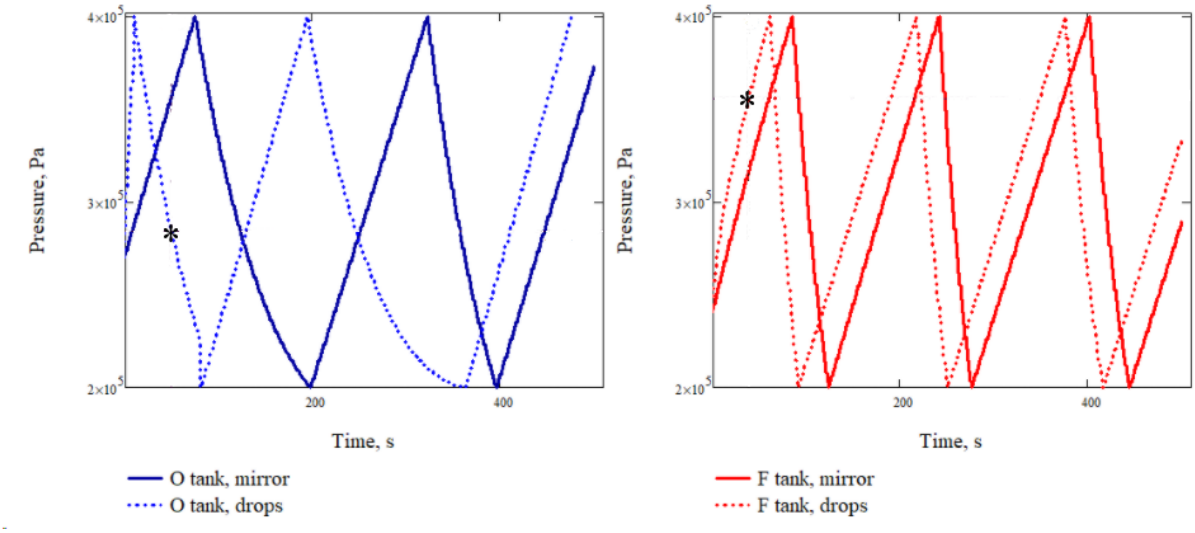

a) b)

Figure 3. Pressure change in O, F tanks for 2 boundary conditions types.

As it follows from the results shown in figure. 3:

– for the boundary condition “drop”, complete oxygen (figure 3a) and kerosene (figure 3b) evaporation occurs before the moment indicated by “*”. After this point in time, pressure will be gained in the tanks O, F only due to the input of HC;

– for the boundary condition “mirror”, the complete oxygen (figure 3a) and kerosene (figure 3b) evaporation occurs within a predetermined time T_{giv} = 500 seconds;

– variants of boundary conditions (“mirror”, “drop”) significantly affect the pressure rise rate in the tanks until the first GVM discharge.

The influence of the HC parameters (speed, temperature, mass second flow) on the liquid evaporation mass rate is carried out through thermophysical parameters (14), (15). In figure 4 shows the time variations of the process, the liquid evaporation mass rates, determined in accordance with (17).

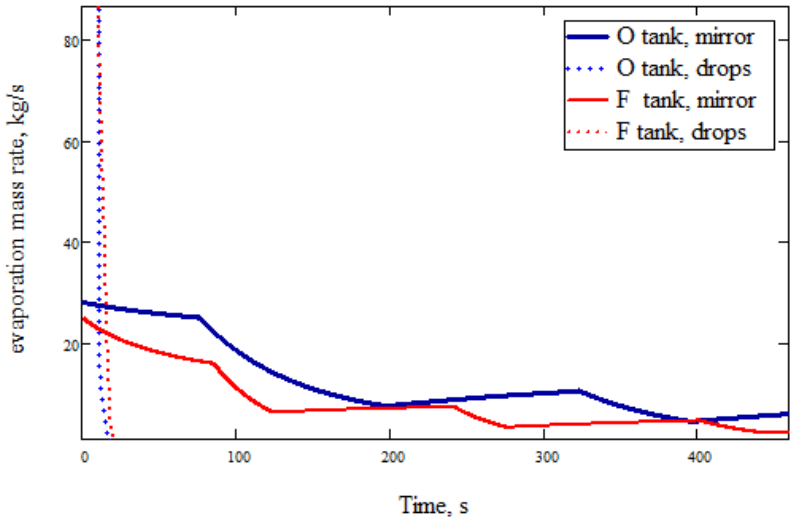

Figure 4. Changes in liquids evaporation mass rates for tanks O and F for two boundary conditions.

As it follows from the above results in figure 4:

– for the variant of the boundary conditions “drop”, the evaporation process of RP liquid residues ends in a significantly smaller time interval (~ 20-25 s), however, the GVM discharge process from the tanks will be for a much longer time interval;

– due to the fact that the evaporation system parameters are chosen from the condition T_{giv} for the variant of the boundary conditions “mirror”, the process lasts 500 seconds.

4.3 Nozzle thrust characteristics

The GVM mass second flow through the gas jet nozzle is determined by the formula [18]:

$$\dot{m}_{out} = F_{out} \cdot \sqrt{2\frac{k}{k-1} p \cdot \rho \cdot \left(\left(\frac{p_1}{p}\right)^{\frac{2}{k}} - \left(\frac{p_1}{p}\right)^{\frac{k+1}{k}} \right)}, \quad (18)$$

where F_{out} is critical area; k is GVM_0 adiabatic index; p_1, ρ_1 are GVM pressure and density at the nozzle exit.

Pressure drop $\frac{p_1}{p}$ varies within 0,02÷0,075 [18].

The GVM flow rate from the nozzle is determined by the formula:

$$w = \sqrt{2\frac{k}{k-1} p \cdot \frac{1}{\rho} \cdot \left(1 - \left(\frac{p_1}{p}\right)^{\frac{k-1}{k}} \right)}, \quad (19)$$

The thrust at heights, where the environment external pressure is negligible, is equal to:

$$P = \dot{m}_{out} \cdot w \quad (20)$$

In figure 5 shows the thrust magnitudes (20) from nozzles for O, F tanks a) and GVM mass flow (18) b) for two boundary conditions variants.

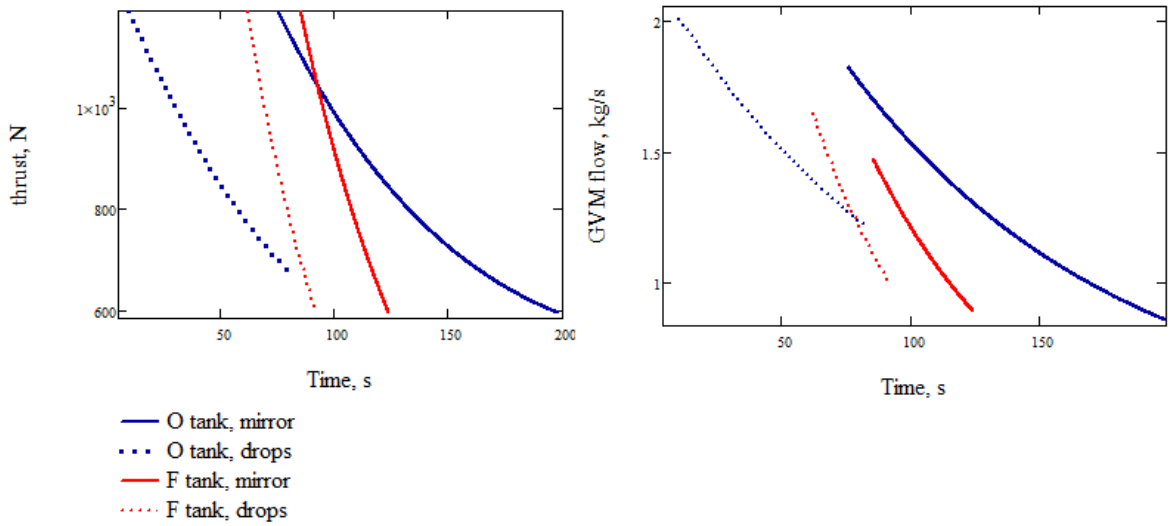

a) b)

Figure 5. The change in the discharge nozzle thrusts magnitude a) and the GVM mass flow on the inteval of the first GVM discharge from the O, F tanks, b) under different boundary conditions.

As follows from the above results in figure 5:

– the boundary conditions practically do not affect the thrust values (figure 5a), however, the achievement of the pressure magnitude in the O, F tanks for the boundary conditions “drop” variant occurs much faster than for the variant “mirror”; a decrease in the thrust magnitude (20) occurs due to a decrease in the mass flow rate (18) and exhaust velocity (19);

– the change nature of the GVM mass flow rate practically does not depend on the boundary conditions variants, however, the maximum values achievement occurs much faster for the boundary conditions “drop” variant, which corresponds to a larger evaporation area.

5. Evaporation system scheme

In figure 6 shows a schematic diagram of the evaporation system placement on ES.

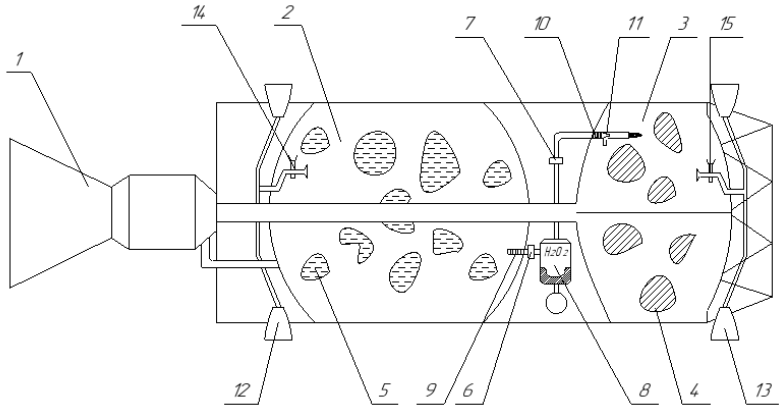

Figure 6. Schematic diagram of the evaporation system placement on ES: 1 – main LRE; 2 – O tank; 3 – F tank; 4 – kerosene liquid residues in the state of a gas-droplet mixture; 5 – oxygen liquid residues in the state of the gas-droplet mixture; 6, 7 – control valves for supplying hydrogen peroxide to O, F tanks; 8 – tank with hydrogen peroxide with a membrane feed system; 9, 10 – catalytic systems for the hydrogen peroxide decomposition in O, F tanks; 11 – injection pump for the GVM supply in the F tank; 12, 13 – GVM discharge gas jet nozzles from O, F tanks; 14, 15 – controlled GVM dump valves from O, F tanks to a gas-reactive stabilization system.

The evaporation system works as follows: after shutting down the LRE 1, in the O 2, F 3 tanks, RP liquid residues 5, 6 can occupy random positions, including those shown in fig. 5. At the same time (possibly with an interval), valves 6, 7 are opened for supplying HP from tank 8 to catalytic decomposition systems 9, 10 located directly in tanks and oriented to supply high-temperature decomposition products to O, F tanks volumes. GVM supply system tank 11 in the nozzle is provided for the possibility of kerosene vapor ignition to achieve the appropriate concentration. After achieving pressures in the tanks O, F, corresponding to the calculated ones for the GVM discharge, adjustable valves 14, 15 open to discharge the GVM into the gas jet nozzles 12, 13.

Table 1 shows the initial data for assessing the evaporation process parameters on the example of the LV "Soyuz 2.1.v" first ES.

Table 1. The evaporation system parameters adopted in the simulation

	Parameter name, dimension	value
1	The heat required amount to heat the helium and RP residues in the O/F tanks, MJ	155/100
2	The HP supply mass flow rate in O/F tanks, kg/s	0,137/0,089
3	HP mass for O/F tanks, kg	68/44
4	Operation time of the evaporation system in O/F tanks, s	500
5	Spherical tank volume for HP, (for R=0,28 m), m^3	0,09
6	The HP tank design mass of AMG-6 with a release membrane, kg	6,7
7	Length, diameter and thickness of pipelines, mm	1000/50/2
8	Control valves mass, kg	3,0
9	The total evaporation system mass, kg	122,3
10	The relative evaporation system mass in the O, F tanks in comparison with the ES “dry” design mass, %	1,3

6. The results discussion

The proposed method for studying the evaporation process parameters of the RP unusable liquid residues based on the thermodynamics law equations using hydrogen peroxide. As boundary conditions for the liquid RP initial state, two variants were considered: the liquid mirror presence in the tank bottom with a constant surface and the liquid droplet distribution in the tank volume. The above equations consider the heat exchange between a) GVM_{HC} and GVM_0 in the O tank, b) GVM_0 with liquid, c) GVM_0 with the O tank wall. The accepted assumptions for determining these GVM characteristics allowed the evaporation process parameters approximate estimates to be obtained. At the same time, the most important characteristic of the convective heat transfer – the heat transfer coefficient, which also belongs to the mass transfer coefficient, – was obtained for the Grashof, Froude criterium corresponding to ground conditions.

The obtained equations for estimating the liquid oxygen evaporation process parameters in the O tank are fully valid for F tank with liquid kerosene residues. In the given example, the oxygen and kerosene evaporation processes parameters are shown.

At the end of the evaporation system operation, 5.5% of RP residues, including 1.2% of unusable oxygen, remained in the tank O, and 0.86% of RP residues, including 0.5% of unusable kerosene, 0.36% of water vapor and oxygen, remained in the tank F.

In [14], the GVM thermophysical parameters definition was considered on the basis of the boundary layer theory and integral ratios of impulses, energy and diffusion under the condition of the liquid RP even distribution over the inner tanks surface and the GVM continuous outflow from the tanks. The comparative analysis of the GVM thermophysical characteristics in the tanks O, F (heat capacity, thermal conductivity and heat transfer) in the evaporation process showed the proximity of the obtained thermophysical characteristics.

Conclusion

1. A method has been developed to study the evaporation process parameters of the unusable liquid RP residues in the ES tanks after turning off the main LRE based on the use of hydrogen peroxide

decomposition products as a heat carrier, which includes the GVM thermophysical parameters assessment, GVM exhaust velocity from the O, F tanks, and the GVM discharge nozzle thrust from O and F tanks with different boundary condition variants of liquid RP residues.

2. The presence of the mode for GVM pressure release through nozzles from the tanks and the mode of pressure gain in the tanks leads to the oscillatory nature of the evaporation process parameters.

3. It is shown that it is possible in principle to efficiently use the method for extracting energy resources contained in unusable liquid RP residues.

The proposed method makes it possible to abandon a significant list and amount of work and, accordingly, save time and money on minimizing unusable liquid RP residues in the operating tanks after main LRE shutdown. The evaporation system mass does not exceed 1.3% of the "dry" ES design mass.

References

[1] Raikunova G G 2014 *Space debris Prevention of space debris* (Moscow) p 188
[2] Kompaniec E, Kuchma L, Podolinny A and Shatrov Ya 1990 *Investigation of ways to reduce areas of incidence of separated parts of missiles* (Moscow) p 164
[3] Andrienko A Ya and Ivanov V P 2009 Improving the energy characteristics of liquid rockets by automatic control means *Physicotechnical bases for managing the expenditure of liquid propellant rockets (Problems of Control)* pp 66–71
[4] Andrienko A I, Balakin S V, Lomtev S M and Portnov-Sokolov Yu P 2003 The problem of measuring the level of propellant on board liquid rockets *Sensors and Systems* pp 46–57
[5] Baranov D A, Makarov Yu N, Shatrov Ya T and Trushlyakov V I 2015 The project of creating an autonomous onboard system for discharging spent stages of launch vehicles to specified areas *Cosmonautics and Rocket Science* **50(84)** pp 76–82
[6] Trushlyakov V I, Lempert D B and Belkova M E 2015 Study of the possibility of using gas-generating compositions to improve the effectiveness of liquid rockets *Combustion and explosion physics* **51** pp 48–54
[7] Trushlyakov V, Shatrov Ya, Sujmenbaev B and Baranov D 2017 The designing of launch vehicles with liquid propulsion engines ensuring fire, explosion and environmental safety requirements of expended stages *Acta Astronautica* **131** pp 96–101
[8] Trushlyakov V and Shatrov Ya 2017 Improving of technical characteristics of launch vehicles with liquid rocket engines using active onboard de-orbiting systems *Acta Astronautica* **138** 19-27
[9] Baranov D A, Lempert D B, Trushlyakov V I and Shatrov Ya T 2017 Development of an onboard evaporation system for non-producing residual liquid propellant in the tanks of the separating part of the LV stage *Astronautics and Rocket Engineering*, **6** pp 93–103
[10] Belyaev N M 1976 *Systems of pressurization of propellant tanks of rockets* (Moscow: Engineering) p 335
[11] Trushlyakov V I, Shalay V V and Shatrov Ya 2004 T *Reducing the anthropogenic impact of rocket launch vehicles on the liquid toxic components of rocket propellant on the environment*, ed. V I Trushlyakov (Omsk: Publishing house OGTU) p 220
[12] Rui Ma, Yu-ting Wu and Chun-xu Du Yan 2018 Experimental Study of Weightless Effect on Small Vapor Compression *Microgravity Sci. and Technology* **30** p 977–985
[13] Chen Xue, Zhu Zhi-Qiang and Liu Qiu-Sheng 2015 Thermodynamic Behaviors of Macroscopic Liquid Droplets Evaporation from Heated Substrates *Microgravity Sci. and Technology* **27** pp 353–360
[14] Fang Wang, Rui Liu, Min Li, Jie Yao and Jie Jin 2018 Kerosene evaporation rate in high temperature air stationary and convective environment *Fuel* pp 582 – 590
[15] Zhao J F 2010 Two-phase flow and pool boiling heat transfer in microgravity *Multiphase Flow* **36** pp 135–143
[16] Trushlyakov V and Lavruk S 2015 Theoretical and experimental investigations of interaction of hot gases with liquid in closed volume *Acta Astronautica* **109** pp 241-247
[17] Gershuni G Z and Zhukhovitsky E M 1972 *Convective stability of an incompressible fluid* (Moscow: Science) p 393

[18] Sinyarev G B and Dobrovolsky M V 1955 *Liquid rocket engines* (Moscow: State publishing house of defense industry) p 499
[19] Lukanin V N 2008 *Heat engineering: study guide for universities* ed. V N Lukanin, M G Shatrov and G M Kamfer et al. (Moscow: Higher School) p 671
[20] Shalai V V, Trushlyakov V I and Kudentsov V Yu 2014 Simulation of heat and mass transfer processes during gasification of liquid propellant residues in missile tanks *Thermal problems in engineering* **6** pp 67–74
[21] Fedorov A V, Bedarev I A and Lavruk S A 2018 Determination of the flow field in the propellant tank of the rocket engine after the mission has been completed // *Engineering Physics Journal* **91** pp 345–353
[22] Vargaftik N B 1972 *Handbook of the thermophysical properties of gases and liquids* (Moscow: The science. The main editors of physical and mathematical literature) p 720
[23] Kutateladze S S 1958 *Handbook of heat transfer* (Moscow: GEI) p 418

Acknowledgements
The research was supported by the grant of the Ministry of education and science of the Russian Federation "Improvement of environmental safety and economic efficiency of launch vehicles with main liquid rocket engines", No. 9.1023.2017 PCH.